Magnetic Properties of Some Type-II Alloy Superconductors near the Upper Critical Field*

W. A. FIETZ† AND W. W. WEBB
Department of Engineering Physics and Laboratory of Atomic and Solid State Physics, Cornell University, Ithaca, New York

(Received 23 March 1967)

Parameters pertinent to the magnetic properties of type-II superconductors near the upper critical field H_{c2} [namely, the generalized Ginzburg-Landau parameters κ_1 and κ_2, and the functions $h^*=H_{c2}/(-dH_{c2}/dt)_{t=1}$] have been obtained from magnetization measurements on a series of niobium-titanium alloys. The range of electron-transport mean free paths, from $0.1\xi_0$ to about $15\xi_0$ (where ξ_0 is the coherence length in pure Nb), effectively spans the range from the clean to the dirty limit, with annealed and cold-worked specimens at temperatures between $0.13T_c$ and T_c. It was found that both κ_1 and κ_2 increased with decreasing temperature in all alloys and that the magnitude of the increase was 20–50% higher than expected from existing theory. The experimental value of the parameter $H_{c2}/(dH_{c2}/dt)$ at $T=T_c$ various with impurity roughly as expected in Ginzburg-Landau theory. Defects generated by cold work enhanced the increase of κ_1 at low temperatures.

INTRODUCTION

THE magnetic properties of type-II superconductors have been studied intensively since Abrikosov[1] first obtained a theoretical description from a solution of the Ginzburg-Landau[2] equations. Later Gor'kov[3] showed that these equations followed from the microscopic theory of Bardeen, Cooper, and Schrieffer.[4] Since the Ginzberg-Landau equations were restricted to a small range of validity near the critical temperature T_c, other theorists,[5] following Gor'kov, have attempted to extend the region of validity or to find more general descriptions of type-II superconductors that relate to the microscopic characteristics of the material such as the Fermi velocity v_F, the density of states at the Fermi surface $N(0)$, and the electron mean free path l. Most of the theoretical results pertain to the region of the second-order transition near the upper critical field H_{c2} where the gap function Δ is small and forms a convenient expansion parameter. Therefore, experimental data on temperature and composition dependence of the magnetic properties of type-II superconductors that are associated with the upper critical field, the upper critical field H_{c2}, and the slope of the magnetization curve near the upper critical field $(dM/dH)_{H_{c2}}$ are of particular interest. It is the object of this paper to present some experimental measurements of such magnetic properties on a series of niobium base alloys over a range of compositions between the "clean" and the "dirty" limits of electron mean free path.

It is customary to present theoretical results based on a generalization of the Ginzburg-Landau theory in terms of several generalized parameters κ_1, κ_2, and κ_3 which reduce to the usual Ginzburg-Landau parameter κ at T_c. Our data relate to κ_1 which is proportional to H_{c2}, and to κ_2 which is associated with $(dM/dH)_{H_{c2}}$. For convenience, a summary to January 1967 of recent theoretical results on κ_1 and κ_2 in type-II superconductors and their regions of validity are given in Table I. The entire range of temperature and mean free path variation is covered by one or more of the theoretical calculations. These calculations, of course, agree with one another in the regions of overlap except where errors have already been pointed out. Therefore, it appears that a comparison of theory and experiment over a wide range of temperature and mean free path would provide a good test of the basic assumptions common to all these theories, which include spherical Fermi surfaces, isotropic scattering (in most cases), and weak electron-phonon interaction. Effects of p-wave scattering have been included in one calculation covering the entire range. Effects of paramagnetism have been included only in the dirty limit.

Many experimental studies of the upper critical field of type-II superconductors have appeared, and a summary of the experimental situation is given in Table II. However, the data available for comparison with theory are not so abundant as the table might imply because in many cases the necessary microscopic parameters or normal-state properties are not specified, so that comparisons made by estimating these terms and using the published values for others are too imprecise to be useful. Also there are few data covering the intermediate mean free path range and providing the necessary connection between the "pure" and the "dirty" limits.

To provide data covering a wide range of electron mean free path and temperature, we have chosen

* This research was supported by the U.S. Atomic Energy Commission and benefitted from facilities provided by the Advanced Research Projects Agency.

† Present address: Speedway Laboratories, Linde Division, Union Carbide Corporation, Indianapolis, Indiana.

[1] A. A. Abrikosov, Zh. Eksperim. i Teor. Fiz. **32**, 1442 (1957) [English transl.: Soviet Phys.—JETP **5**, 1174 (1947)].

[2] V. L. Ginzburg and L. D. Landau, Zh. Eksperim. i Teor. Fiz. **20**, 1964 (1950).

[3] L. P. Gor'kov, Zh. Eksperim. i Teor. Fiz. **36**, 1918 (1959); **37**, 1407 (1959) [English transls.: Soviet Phys.—JETP **9**, 1364 (1959); **10**, 998 (1960)].

[4] J. Bardeen, L. N. Cooper, and J. R. Schreiffer, Phys. Rev. **108**, 1175 (1957).

[5] L. P. Gor'kov, Zh. Eksperim. i Teor. Fiz. **37**, 833 (1959) [English transl.: Soviet Phys.—JETP **10**, 593 (1960)].

TABLE I. A tabulation of some of the recent theoretical work pertaining to type-II superconductors, especially to magnetic properties near the upper critical field H_{c2}.

Parameter	Pure limit	General case	Dirty limit
$\kappa_1(t)$	Gor'kov[a]	Helfand and Werthamer[b]	Shapoval[c]
		Eilenberger[d]	Maki[e]
		Tewordt[f] (near T_c only)	Maki[g]
			Werthamer, Helfand, and Hohenberg[h]
			de Gennes[i]
$\kappa_2(t)$	Maki and Tsuzuki[j]	Eilenberger[d]	Maki[k]
		Neuman and Tewordt[l] (near T_c only)	Maki[g]
			Caroli, Cyrot, and de Gennes[m]

[a] See Ref. 5.
[b] See E. Helfand and N. R. Werthamer, Phys. Rev. Letters **13**, 686 (1964). See also Ref. 10.
[c] Contains an error pointed out by N. R. Werthamer. Rev. Mod. Phys. **36**, 116 (1964). See also E. A. Shapoval, Zh. Eksperim. i Teor. Fiz. **41**, 877 (1961) [English transl.: Soviet Phys.—JETP **14**, 628 (1962)].
[d] Calculated for s-wave plus p-wave scattering. See G. Eilenberger, Z. Physik, **190**, 142 (1966). See also Ref. 13.
[e] Reference 8.
[f] Reference 12.
[g] Includes effects of spin paramagnetism. See K. Maki, Physics **1**, 127 (1964).
[h] Includes electron spin and spin-orbit effect. See Ref. 11.
[i] See P. G. de Gennes, Phys. Kondensierten Materie **3**, 79 (1965).
[j] K. Maki and T. Tsuzuki, Phys. Rev. **139**, A868 (1965).
[k] Contains an error brought out by C. Caroli, M. Cyrot, and P. G. de Gennes, Solid State Commun. **4**, 17 (1966). See also Ref. 8.
[l] L. Neumann and L. Tewordt, Z. Physik **191**, 73 (1966).
[m] C. Caroli, M. Cyrot, and P. G. de Gennes, Solid State Commun. **4**, 17 (1966).

niobium-titanium alloys with compositions varying between pure niobium and 12 at.% titanium. This system has the property that while the electron mean free path varies between about $0.1\xi_0$ and $15\xi_0$, the thermodynamic critical field $H_c(T)$ and the critical temperature T_c are nearly constant. Thus, in this system it is possible to consider the electronic mean free path l as a nearly independent variable, while the basic superconducting parameters remain nearly invariant. Electron-phonon coupling is thought to be of intermediate strength in this system. Except for the highest alloy, H_{c2} is low enough that paramagnetic effects should be nelgigible.

EXPERIMENTAL

Methods

The magnetic properties were obtained from data on the applied field dependence of the magnetization of long cylindrical samples of each alloy, measured by electronic integration of the potentials developed in 25 000-turn pickup coils during a slow sweep of the applied magnetic field. This technique, as previously described by one of us,[6] provided a direct continuous plot of the magnetic moment versus applied field, with an over-all accuracy better than 2%. Calibration of the magnetic moment in terms of the magnetization of a specimen of negligible demagnetization factor was accomplished by making use of the initial diamagnetic slope of each specimen after cooling in zero field. A high uniformity magnetic field (0.05% over 6 cm along the axis) was provided by a 40-kOe superconducting solenoid powered by a self-ramping current regulator.[6] Representative curves for two samples are shown in Fig. 1.

The specimen and measuring coils were arranged inside a vacuum-insulated can in which the temperature could be varied between 1.2 and 15°K either by pumping on liquid helium in the can, or by electrical heating with a resistance coil in the presence of an exchange gas. Temperature was measured on a calibrated carbon resistor in thermal contact with the specimen. This resistor formed the sensing element in a feedback system which maintained the temperature within 0.1°K during measurements above 4.2°K. Temperatures below 4.2°K were set by a manostat controlling the vapor pressure within the can, and fluctuations were less than 0.01°K.

Resistivity and resistivity ratios of the alloys in the normal state were measured by observing the voltage drop along the specimen in the presence of a small transport current while in a magnetic field sufficient to quench superconductivity, or in one case while at a temperature slightly above the transition temperature.

The alloy specimens were prepared under the supervision of Professor J. L. Gregg in a facility of the Materials Science Center at Cornell University. Rods about 6 cm long and 0.37 cm in diameter were swagged without intermediate anneal from ingots 1.25 cm in diameter. The ingots were prepared by repeatedly arc melting high-purity materials which had been electron-beam-zone refined. Chemical analyses of the specimens after their final treatment are given in Table III.

The cold-worked samples were chemically polished to a diameter of 0.36 cm to remove the surface damage in preparation for the recording of hysteretic magnetization curves representative of the bulk properties. Only the values of the upper critical field H_{c2} for these specimens were used in this study. Results of a detailed investigation of their hysteretic properties will be published elsewhere.

Annealed specimens were prepared, after a chemical polish, by induction heating to within 100°C of the melting point for 3 min, then holding at about 1800°C for 30 min in a vacuum always better than 2×10^{-6} Torr. This procedure minimized evaporation of titanium yet sufficed to produce nearly reversible magnetization curves. After the anneal, the diameter was reduced another 0.01 cm by electrolytic polishing at −70°C in an electrolyte containing 93 ml methanol, 5 ml

[6] W. A. Fietz, Rev. Sci. Instr. **36**, 1306 (1965).

TABLE II. A tabulation of some of the recent experimental work on type-II superconductors pertaining to magnetic properties near the upper critical field H_{c2}. Materials to which data apply are given in parentheses.

Parameter	Electronic Mean Free Path: pure limit	intermediate	dirty limit
$\kappa_1(t)$ or $H_{c2}(t)$	McConville and Serin[a] (Nb)	McConvllle and Serin[a] (Nb)	McConville and Serin[a] (In–Bi) (Nb–Ta)
	Skinner, Rose, and Wulff[b] (Nb)		Shapira and Neuringer[c] (Nb–Ti)
	Finnemore, Stromberg, Swenson[d] (Nb)		Jones, Hulm and Chandrasekhar[e] (Nb–Ti) (Nb–Zr)
	Rosenblum, Autler, and Goosen (Nb)	Rosenblum, Autler and Gooen[f] (Nb)	Rosenblum, Autler and Gooen[f] (Nb)
	Radebaugh and Keesom[g] (V)		Joiner and Blaugher[h] (Mo–Re)
	Strnad and Kim[i] (Nb)		Kinsel, Lynton, and Serin[j] (In–Bi)
			Bon Mardion, Goodman, and Lacaze[k] (Pb–Tl)
			Strnad and Kim[i] (Nb)
$\kappa_2(t)$	McConville and Serin[a] (Nb)	McConville and Serin[a] (Nb)	McConville and Serin[a] (Nb)
	Skinner, Rose, and Wulff[b] (Nb)		Bon Mardion, Goodman, and Lacaze[k]
	Finnemore, Stromberg and Sewnson[d]		
	Radebaugh and Keesom[g]		

[a] Reference 21.
[b] Reference 22.
[c] Reference 23.
[d] Reference 23.
[e] Reference 27.
[f] Reference 24.
[g] Reference 25.
[h] Reference 29.
[i] Reference 26.
[j] Reference 30.
[k] Reference 31.

H_2SO_4, and 2 ml HF, given by Nembach.[7] This was the only treatment found that would remove the titanium-depleted surface layer without introducing additional magnetic hysteresis by chemical action at the surface.

The depth of the surface treatments described above was determined to be sufficient to attain radial uniformity within the specimens by observing that no further change occurred in the magnetic properties as more material was removed.

TABLE III. Typical chemical and spectroscopic analyses of alloys used in this study.

Specimen (nominal atomic % Ti)	Titanium (atomic percent[a])	Composition: Oxygen ppm[b]	Carbon ppm	Tantalum ppm	Other ppm
Annealed					
0.5 Ti	0.72				
1.5 Ti	1.5				
		7–28	115–160	100–350	10–50
4.5 Ti	4.0				
9.0 Ti	8.1				
Worked					
0.5 Ti	0.96				
1.5 Ti	1.5				
4.5 Ti	3.6	80–120	110–165	100–350	10–50
9.0 Ti	9.1				
12.5 Ti	12.0				

[a] Uncertainty believed to be 10% of figure given.
[b] Typical values in ppm by weight. Range of values was obtained in testing about 10 different samples of varying compositions including pure Nb.

[7] E. Nembach, Phys. Status Solidi **13**, 543 (1966).

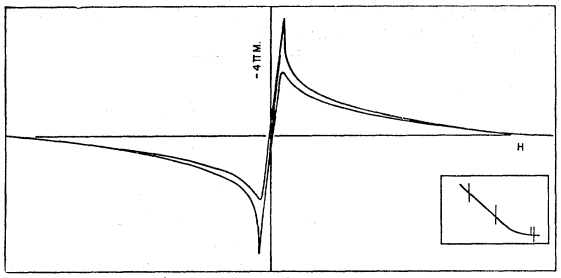

FIG. 1. An example of magnetization data obtained by electronic integration of induced signals proportional to the time rate of change of M and H during field sweeping. The inset shows a section of the curve near H_{c2} with the vertical scale expanded by a factor of 10. In the expanded section, the normal-state susceptibility may be determined from the slope of the curve above H_{c2}.

Error Analysis

Instrumentation errors inherent in the process of obtaining and recording the magnetization curves are well known and were of the order of 1–2% of the maximum magnetization for the most part. Other uncertainties may arise in obtaining acceptable values for the three quantities taken from the magnetization curves, H_c, H_{c2}, and $(dM/dH)_{H_{c2}}$ because of hysteretic transitions which are not sharp, temperature variations, surface effects, and nonuniformity of magnetic field or specimen composition.

The values of H_c were obtained from the area under an increasing magnetization curve starting with no trapped flux in the specimen. The hysteresis amounted to about 5–20% of the area under the increasing field curves, but analysis of possible hysteresis mechanisms suggests that the true value for H_c lies closer to the values lying under the increasing field curves than to the average of the two areas under increasing and decreasing field curves. Comparison with the results of Finnemore, Stromberg, and Swenson on very pure niobium shows that our values of H_c for niobium are about 5% higher. We assume that our values for H_c represent an upper limit and expect an error of about 0 to +6%. This source of error may lead to underestimates of the values of κ_1 and κ_2.

The values for H_{c2} are reliable to within instrumentation errors of ~1% except for high titanium alloys near $T=T_c$ where the fractional uncertainties increase to about 5% due largely to temperature uncertainties. Similarly the values for $(dM/dH)_{H_{c2}}$ are well known except in the vicinity of T_c in the high titanium specimens. Although uncertainties of most values of κ_1 and κ_2 are less than 2%, individual normalized values of $\kappa_1(t)/\kappa_1(1)$ and $\kappa_2(t)/\kappa_2(1)$, where $\kappa_1(1)$ and $\kappa_2(1)$ are the limiting values at $t=T/T_c=1$ have uncertainties up to 5–8% because of the uncertainty of $\kappa_1(1)$ and $\kappa_2(1)$ which depend on an extrapolation of data near $t=1$.

Effects on speciman temperature due to heat evolved during the magnetization cycle were investigated by disabling the temperature controller and observing the temperature changes with a constant power input to the heater. This variation was found to be less than 0.3°K and was easily corrected by the feedback system. The magnetoresistance of the carbon resistor was found to contribute an error less than 0.1°K, even in the highest fields used, so was not compensated. The over-all temperature error of 0.1°K limited accuracy only near T_c.

Reduction of the field sweep rate by a factor of 10 from its normal value of about 150 Oe/sec had no measurable effect upon the magnetization data, so it was concluded that rate effects were unimportant.

CALCULATIONS

In this section, the definitions and procedures needed for comparison of the experimental data on type-II superconductors with theory are summarized. Maki[8] defined two parameters $\kappa_1(t)$ and $\kappa_2(t)$ to describe properties near the upper critical field. Helfand and Werthamer have, in addition, introduced a normalized parameter h^* to describe the temperature dependence of $H_{c2}(t)$. The normalized temperature is $t=T/T_c$.

The generalized Ginzburg-Landau parameters $\kappa_1(T)$ and $\kappa_2(T)$ are defined in terms of the measurable quantities H_c, H_{c2}, and dM/dH by the relationships

$$H_{c2}(t)=\sqrt{2}\kappa_1(t)H_c(t) \tag{1}$$

and

$$-4\pi(dM/dH)_{H_{c2}}=[\beta(2\kappa_2^2(t)-1)]^{-1}, \tag{2}$$

where $\beta=1.16$ for the triangular fluxoid lattice of Kleiner, Roth, and Autler,[9] which will be assumed hereafter. The parameter defined by Helfand and Werthamer,

$$h^*(t)=H_{c2}(t)/(-dH_{c2}/dt)_{t=1}, \tag{3}$$

provides an additional route to the analysis of data on H_{c2}, independent of the measurements of $H_c(t)$. They give values of $h^*(t)$ for $0\leq t\leq 1$ and independently for $(-dH_{c2}/dt)_{t=1}$.

The upper critical field H_{c2} and the slope $(dM/dH)_{H_{c2}}$ are taken directly from the reversible magnetization data plotted by an x-y recorder and the bulk critical field H_c is obtained from the area under the curve as the magnetic field is increased from zero to above H_{c2}. Thus three experimental quantities are independently determined as functions of temperature. The temperature dependence of κ_1, κ_2, and h^* may thus be obtained for each alloy composition from a series of magnetization curves taken at various temperatures. However, for the cold-worked specimens only H_{c2} is measurable because their magnetization curves are not reversible. By assuming that H_c is not appreciably changed by cold-working, the parameter $\kappa_1(T)$ can be calculated for each deformed alloy using the values of H_c for corresponding annealed specimens of the same composition.

[8] K. Maki, Physics **1**, 21 (1964).
[9] W. H. Kleiner, L. M. Roth, and S. H. Autler, Phys. Rev. **133**, A1226 (1964).

Each alloy is characterized by another independent variable, the electron mean free path l. Since the electron mean free path varies strongly with concentration of titanium, interstitial impurities, and dislocation density, it is necessary to measure the resistivity of each individual specimen in order to obtain a measure of its mean free path. A quantity ρ proportional to the ratio of the superconducting coherence length to the electron mean free path was introduced by Gor'kov to characterize the "purity" of a superconductor. This quantity is identical to λ used by Werthamer *et al.*,[10,11] α used by Tewordt,[12] and the ratio ξ/l used by Eilenberger.[13] This quantity is here designated

$$\rho=\hbar/(2\pi K_B T_c \tau)=0.882\xi_0/l, \qquad (4)$$

where T_c is the superconducting transition temperature, ξ_0 is the usual coherence length of a pure superconductor as given by Gor'kov, $\hbar$ and k_B are Planck's and Boltzmann's constants, respectively, and τ and l are the relaxation time and mean free path for normal-state transport processes.

Gor'kov[3] has calculated the ratio κ/κ_0 in the limit $T\rightarrow T_c$ as a function of the impurity parameter ρ where κ_0 is the Ginzburg-Landau parameter in the clean limit. His results were presented in the form

$$\kappa/\kappa_0=[\chi(\rho)]^{-1} \qquad (5)$$

Using Eq. (5), values of ρ can thus be determined from measurements of κ provided that κ_0 is known. Expressions for κ_0 in terms of experimentally observable parameters[14] involve, as another electronic-structure-dependent parameter, the effective area of the Fermi surface S. Thus, it is useful to introduce the ratio

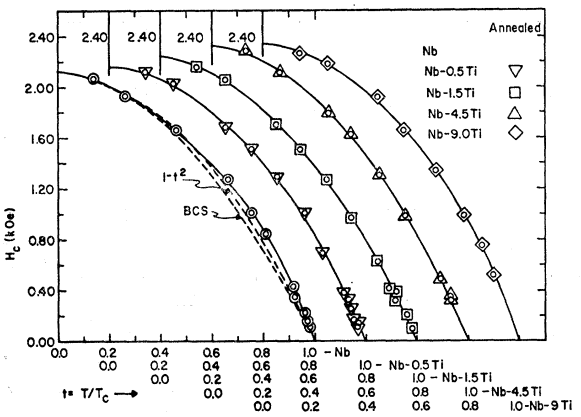

FIG. 2. The theromdynamic critical fields $H_c(t)$ determined from measurements of the areas under the magnetization curves recording during field increases. For clarity the horizontal scale for each curve has been displaced. The higher dashed curve has the form $1-t^2$ and the lower one is the BCS function.

[10] E. Helfand and N. R. Werthamer, Phys. Rev. **147**, 288 (1966).
[11] N. R. Werthamer, E. Helfand, and P. C. Hohenberg, Phys. Rev. **147**, 295 (1966).
[12] L. Tewordt, Z. Physik **180**, 385 (1964).
[13] G. Eilenberger, Phys. Rev. **153**, 584 (1967).
[14] B. B. Goodman, IBM J. Res. Develop. **6**, 63 (1962); Phys. Letters **1**, 215 (1962).

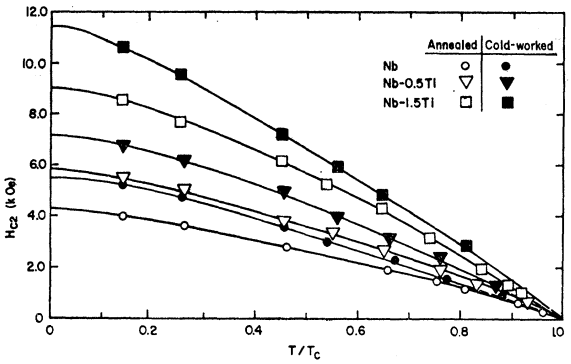

(a)

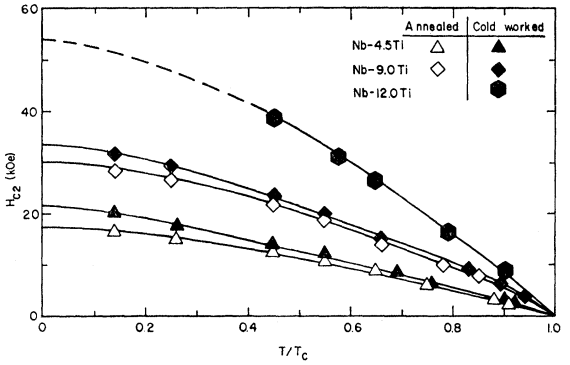

(b)

FIG. 3. The upper critical fields $H_{c2}(t)$ obtained from the magnetization curves, (a) low field alloys (b) high field alloys.

S/S_f where S is the area of the Fermi surface and S_f is the area calculated for free electrons at the same density. The quantity κ_0 has been given in a useful form by Berlincourt and Hake[15] as

$$\kappa_0=1.61\times10^{24}T_c\gamma^{3/2}/[n^{4/3}(S/S_f)^2], \qquad (6)$$

where n is the effective electron density in electrons per cm^3 and γ is the electronic specific heat coefficient in erg cm^{-3} deg^{-2}. Goodman[16] has given a convenient review of the formulas of Ginzburg-Landau theory in a form in which the Fermi surface area S is explicit.

The value of κ_0 is known for pure niobium to be about 0.80. Using $\kappa_0=0.80$, $n=5$ electrons per atom and $T_c=9.2$°K an effective value of S/S_f can be calculated for niobium. This procedure yields $S/S_f=0.77$ or $(S/S_f)^2=0.6$. Values of κ_0 for the alloys may be calculated with Eq. (6) by assuming that S/Sj is independent of composition, using experimental values of γ and T_c and assuming that n is proportional to the average valence; 5 for Nb, 4 for Ti.

The factor $(S/S_f)^2$ may perhaps best be regarded as an adjustable parameter of uncertain meaning that compensates for quantitative inadequacies of the customary formulas connecting normal state and superconducting properties in the Ginzburg-Landau clean

[15] T. G. Berlincourt and R. R. Hake, Phys. Rev. **131**, 140 (1963).
[16] B. B. Goodman, Rept. Progr. Phys. **29**, 445 (1966).

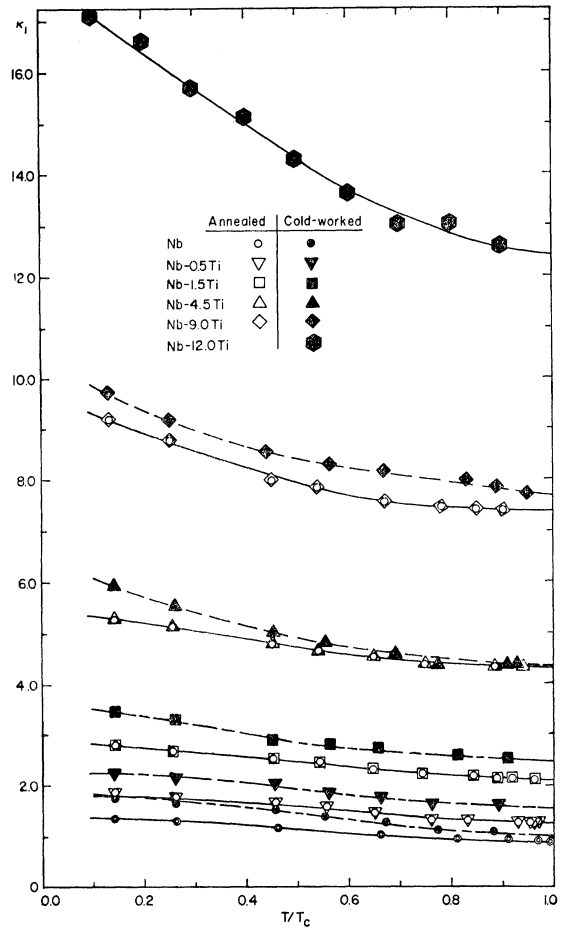

FIG. 4. $\kappa_1(t)$ for all specimens, annealed and cold-worked, as calculated using Eq. (1) of the text and the data obtained from the magnetization curves. $H_c(t)$ for the cold-worked specimens was assumed to be equal to that of annealed specimens of the same composition.

limit. Uncertainties in the choice of values of n and γ for the alloys, and the assumption that the various averages over the Fermi surface of the Fermi velocity v_F and v_F^{-1} are equivalent, are implicit in our value of S/S_f obtained by use of Eq. (6).

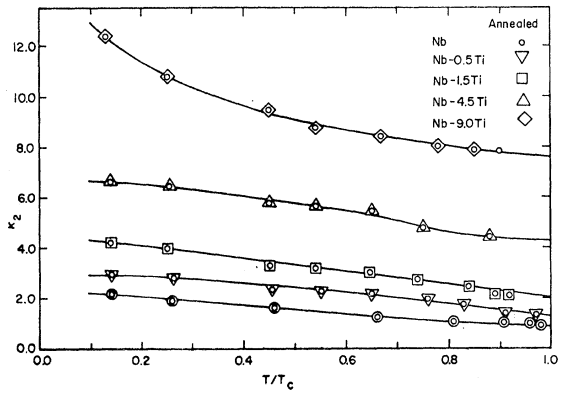

FIG. 5. $\kappa_2(t)$ for the annealed specimens calculated using Eq. (2) of the text and the measured values of the slope of the magnetization curve at H_{c2}.

Combination of Eq. (5) and Eq. (6) yields a formula

$$X(\rho)=1.61\times10^{24}T_c\gamma^{3/2}/[n^{4/3}\kappa(S/S_f)^2] \quad (7)$$

by which ρ can be determined from measured values of κ with the help of a plot of Gor'kov's function $X(\rho)$.[3]

The impurity parameter can also be calculated from the normal-state residual resistivity ρ_n independent of the measurements of κ. Starting from the same formulation of the properties of normal and superconducting state one finds

$$\rho=8.85\times10^3\gamma^{1/2}\rho_n/\kappa_0, \quad (8)$$

where γ is in erg cm^{-3} deg^{-2} and ρ_n is in Ω cm. Again the equivalence of averages of the Fermi velocity over the Fermi surface has been assumed. Insertion of Eq. (6) for κ_0 into Eq. (8) yields

$$\rho=5.5\times10^{-21}[\rho_n n^{4/3}/T_c\gamma](S/S_f)^2. \quad (9)$$

The values of ρ obtained from Eq. (8) and values of κ_0 can be combined to calculate values of κ using Gor'kov's relation, Eq. (5). If the data and the model

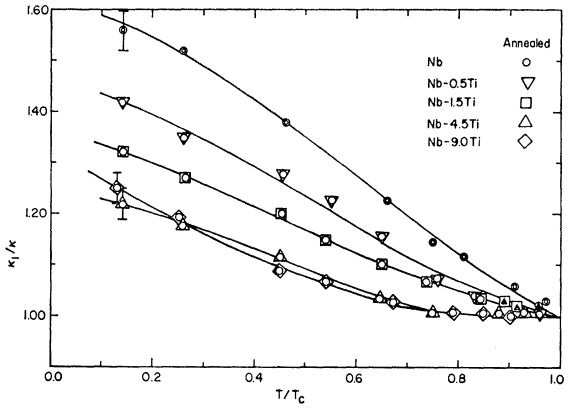

FIG. 6. The normalized function $\kappa_1(t)/\kappa(1)$ for the annealed specimens. The value for the normalizing parameter $\kappa(1)$ is the limiting value of κ_1 as $t\to1$. The error bars are typical for all points and include the uncertainty in $\kappa(1)$.

are adequate, the calculated values of κ obtained this way should agree with the experimental values obtained with Eq. (7). However, the values of κ given by Eq. (5) using Eq. (8) for ρ are compared with the measured values of κ in Table IV and deviations up to 25% are found at intermediate values of ρ. Accordingly, determinations of ρ from measured values of κ using Eq. (7) differ somewhat from values calculated from the residual resistivity using Eq. (9).

Another interesting formula for ρ is obtained by combining Eq. (5) and Eq. (8) to eliminate κ_0 entirely, yielding ρ in terms of $\gamma^{1/2}$, ρ_n and κ as

$$\rho X(\rho)=8.85\times10^3\gamma^{1/2}\rho_n/\kappa. \quad (10)$$

Use of measured values of κ and ρ_n, and γ as estimated from experiment yields substantially smaller values of ρ in the dirty limit than the formulas involving κ_0. No explicit assumptions about n and S/S_f are involved

in this calculation of ρ since these quantities have been eliminated.

In Table IV the relevant data are listed for the alloys measured. Alloys are identified by nominal composition and the actual analyses are given in Table III. The critical temperatures T_c and the normal state resistivity ρ_n were measured directly, and limiting values of the measured quantities $H_c(T=0)$, $\kappa(t=1)$ and $(dH_{c2}/dt)_{t=1}$ were also deduced from the experimental data.

The electronic specific-heat coefficients γ were estimated from the data on pure niobium[17] assuming the small change with compositions to be the same as that observed in vanadium-titanium alloys.[18] The values of ρ listed in column 6 were calculated using Eq. (9) and with the measured values of ρ_n and T_c and values of S/S_f, n and γ discussed above. The corresponding values of κ calculated from Eq. (5) are listed in column 7 for comparison with the measured values of κ given in column 8. Values of ρ calculated from the measured values of κ and ρ_n with γ using Eq. (10) are listed in column 9 and those calculated using measured values of κ and Eq. (7) are given in column 10. For comparison with the measured values of $H_c(0)$, column 12, the values given by the BCS relationship

$$H_c(0)=2.24\gamma^{1/2}T_c \qquad (11)$$

using the tabulated values of γ and T_c are given in column 11 for the annealed alloys.

The uncertainties involved in determining some of these quantities are discussed in preceding sections and are summarized in Table IV.

RESULTS

The basic features of the data on $\kappa_1(t)$, $\kappa_2(t)$, and $h^*(t)$ over a range of reduced temperature $t=T/T_c$ from 0.13 to 1, for a set of Nb-Ti alloys whose electronic mean free path varied between about $0.1\xi_0$ and $15\xi_0$ are first summarized below:

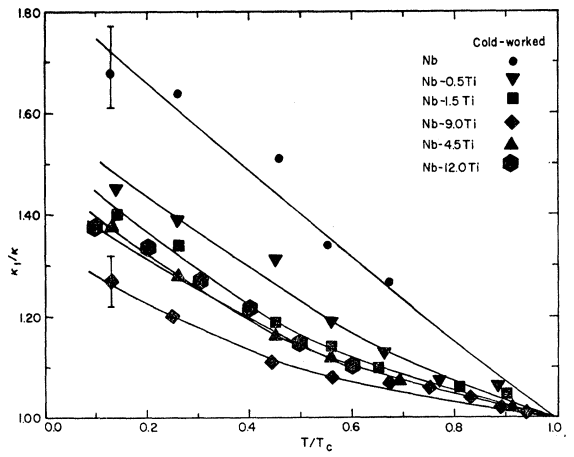

FIG. 7. The normalized function $\kappa_1(t)/\kappa(1)$ for the cold-worked specimens.

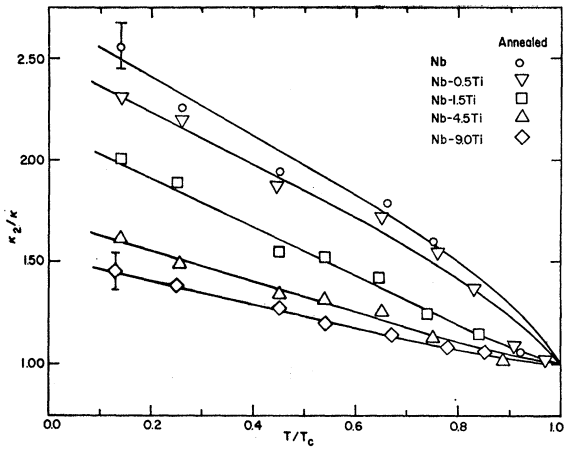

FIG. 8. The normalized function $\kappa_2(t)/\kappa(1)$. The normalizing parameter $\kappa(1)$ is the limiting value of κ_2 as t approaches 1 and for these specimens is identical to that obtained from the limiting value of κ_1.

(1) The thermodynamic critical field data on all the alloys yield, within experimental error, the parabolic temperature dependence $H_c(t)=H_c(0)(1-t^2)$, with possibly higher values at $0.5<t<1$.

(2) The magnitudes of $\kappa_1(t)$ and $\kappa_2(t)$ both increase with decreasing temperature for all alloys tested, and this increase is significantly greater than predicted by the existing theory.

(3) The limiting values of $\kappa_1(t)$ and $\kappa_2(t)$ appear to coincide within the experimental error of a few percent at $T=T_c$ to a value close to Gor'kov's prediction for all values of ρ.

(4) The variation with mean free path of κ_1 and κ_2 at low temperatures also qualitatively agrees with the theory, but again the measured values are consistently larger in magnitude and appear to rise somewhat more sharply than expected below $\rho=1$.

(5) Cold-worked alloys show a stronger temperature dependence of $\kappa_1(t)/\kappa_1(1)$, with consistently higher values of this ratio for all values of ρ.

(6) The quantity $h^*(t)$ agrees within the uncertainties of the data, with the calculation of Werthamer and Helfand (neglecting spin-orbit effects) except for the highest titanium alloy in which spin-orbit effects may begin to be significant. Possibly, however, there is a small systematic deviation, with the purest specimens yielding slightly higher $h^*(t)$ than predicted.

(7) The observed values of the quantity $(dH_{c2}/dT)_{T_c}$ agree in general form with values calculated by Werthamer and Helfand as a function of ρ but appear to deviate systematically.

These results are illustrated in Figs. 2 through 12.

Figure 2 shows the thermodynamic critical fields $H_c(t)$ obtained from the increasing magnetization curve for our specimens. Results for each specimen are displaced horizontally for clarity. With the data on pure niobium, a dashed curve showing the BCS temperature depend-

[17] H. A. Leupold and H. A. Boorse, Phys. Rev. **134**, A1322 (1964).

[18] C. H. Cheng, K. P. Gupta, E. C. van Reuth, and P. A. Beck, Phys. Rev. **126**, 2030 (1962).

TABLE IV. Pertinent parameters of the alloys studied. See text. Estimated errors of experiments are given in top row and previously published data on pure niobium are given in the bottom two rows of the table (Refs. 21 and 23). Parentheses indicate that the estimated error is double the column estimate.

1 Specimen	2 T_c meas. (K°)	3 ρ_n (ohm cm)	4 γ (erg cm^{-3} deg^{-2})	5 κ_0 calc. Eq. 6	6 ρ calc. Eq. 9	7 κ calc. Eq. 5	8 κ meas.	9 ρ calc. Eq. 10	10 ρ calc. Eq. 7	11 $H_c(0)$ calc. (Oe)	12 $H_c(0)$ meas. (Oe)	13 $(dH_{c2}/dt)_{t=1}$ meas. (kOe)
Estim. Error	±0.1	±10%	±8%	...	...	...	±8%	...	...	...	$^{-0}_{+6\%}$	±10%
Annealed												
Nb	9.2	7.3×10^{-8}	7.0×10^{3}	0.80	0.06	0.84	0.9	0.06	0.13	1860	2120	6.1
Nb-0.5 Ti	9.1	4.9×10^{-7}	7.1×10^{3}	0.83	0.38	1.1	1.3	0.41	0.6	1870	2160	8.3
Nb-1.5 Ti	9.1	1.4×10^{-6}	7.2×10^{3}	0.85	1.12	1.7	2.1	0.93	1.6	1890	2240	13.3
Nb-4.5 Ti	9.15	3.5×10^{-6}	7.5×10^{3}	0.91	3.03	3.4	4.2	1.5	3.9	1950	2330	26.6
Nb-9.0 Ti	9.2	8.6×10^{-6}	7.9×10^{3}	0.97	7.15	7.3	7.4	5.7	7.3	2000	2360	52.0
Worked												
Nb	9.1	5.9×10^{-7}	7.0×10^{3}	0.80	0.47	1.2	1.1	0.66	0.39	...	...	7.4
Nb-0.5 Ti	9.0	1.0×10^{-6}	7.1×10^{3}	0.83	0.80	1.5	1.6	0.83	1.0	...	...	9.9
Nb-1.5 Ti	9.0	1.9×10^{-6}	7.2×10^{3}	0.85	1.50	2.0	2.5	1.2	2.2	...	...	15.9
Nb-4.5 Ti	9.1	4.6×10^{-6}	7.5×10^{3}	0.91	3.75	4.0	4.4	3.0	4.2	...	...	30.0
Nb-9.0 Ti	9.2	8.9×10^{-6}	7.9×10^{3}	0.97	7.45	7.6	7.7	5.5	7.7	...	...	60.0
Nb-12.5Ti	9.2	(12.3×10^{-6})	8.3×10^{3}	1.0	9.9	10.	12.4	10.	12.5	...	...	84.0
Ms	9.23	2.8×10^{-8}	8.0×10^{3}	...	0.03	...	0.85	...	...	...	2040	4.9
FSS	9.25	7×10^{-9}	7.3×10^{3}	...	0.006	...	0.78	...	...	...	1990	4.8

ence of $H_c(t)$ and one of the form $H_c(t)=H_c(0)[1-t^2]$ are included for reference. The data are consistent with a parabolic temperature dependence within the experimental uncertainty, but seem to deviate systematically to slightly higher fields at high temperatures. Thus, $-(dH_c/dt)_{t\to 1}\geqq 2H_c(0)$ but the equality may be taken as a good fit to about 10%.

In Fig. 3, values of the upper critical field $H_{c2}(t)$ taken from the magnetization curves are shown for all specimens. From these data, values of $\kappa_1(t)$ and $(dH_{c2}/dt)_{T=T_c}$ were determined. The general features are the same for annealed and cold-worked alloys.

The parameters $\kappa_1(t)$ and $\kappa_2(t)$, calculated from the magnetization data using Eq. (1) and Eq. (2) of the previous section, are given in Figs. 4 and 5. Values of $\kappa_1(t)$ for cold-worked and annealed specimens appear in Fig. 4, and the values of $\kappa_2(t)$ for the annealed specimens only appear in Fig. 5. To within the uncertainty of our measurements, κ_1 and κ_2 coincide at a common value $\kappa(1)$ at $T=T_c$. The scatter of individual measurements is about ± 0.05 for small κ up to ± 0.2 for

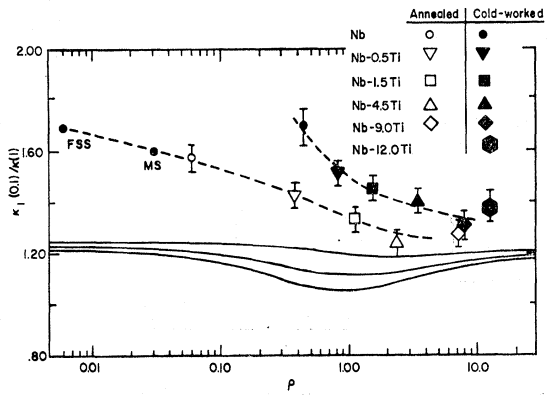

FIG. 9. The mean free path dependence at a fixed temperature $t=0.10$ of the normalized function $\kappa_1(0.10)/\kappa(1)$ for all specimens. Data points for pure niobium from the work of McConville and Serin (MS) and from that of Finnemore, Stromberg, and Swenson (FSS) are included for comparison. The solid lines are the theoretical prediction as calculated by Eilenberger with the ratios 1, 1.5, and 2 for transport mean free path to total mean free path, respectively, from top to bottom.

large κ. However, errors due to residual hysteresis and temperature uncertainty probably limit the precision of individual measurements to $\pm 10\%$. Reproducibility for duplicate specimens falls within this range. However, increase of interstitial impurities changes the κ values and the residual resistivities substantially.

Figures 6 and 7 show the temperature variation of the normalized function $\kappa_1(t)/\kappa(1)$ for the annealed specimens and for the cold-worked specimens, respectively. The normalized function $\kappa_2(t)/\kappa(1)$ for the annealed specimens is given in Fig. 8. The data for low κ appear to display weak inflection points at $t>0.5$, but the precision is inadequate to definitely establish their existence.

For comparison with theoretical calculations in the low temperature limit, the intercept of the best-fit

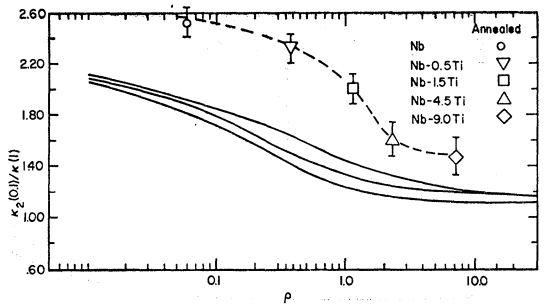

FIG. 10. The mean-free-path dependence of the normalized function $\kappa_2(0.10)/\kappa(1)$. The solid lines are from Eilenberger's calculations, with the ratios of transport mean free path to total mean free path, 1, 1.5, and 2, respectively, from top to bottom.

curves at $t=0.1$ for each specimen have been plotted in Fig. 9 as a function of the impurity parameter calculated using Eq. (9). The temperature $t=0.1$ was chosen instead of $t=0$ because the lowest temperature data were taken at $t\sim 0.13$ and the theoretical results show pronounced curvatures between $t=0.1$ and $t=0$ that might have distorted the comparison at $t=0$. In fact, a comparison at $t=0$ using a linear extrapolation of the data is qualitatively similar to that displayed. Results for both the annealed and the cold-worked specimens are shown on the plot as well as the theoretical values of κ_1/κ at $t=0.1$ obtained from Eilenberger's plots for values of the transport mean free path 1, 1.5, and 2 times the total free path.

The general shape of the observed dependence of $\kappa_1(0.1)/\kappa$ on impurity parameter ρ is in qualitative agreement with the calculations of Eilenberger and of Helfand and Werthamer. However, it is clear that the experimental values are generally higher and the increase at low temperatures is much larger than the theory predictions. Whether the dip in $\kappa_1(0.1)/\kappa$ near

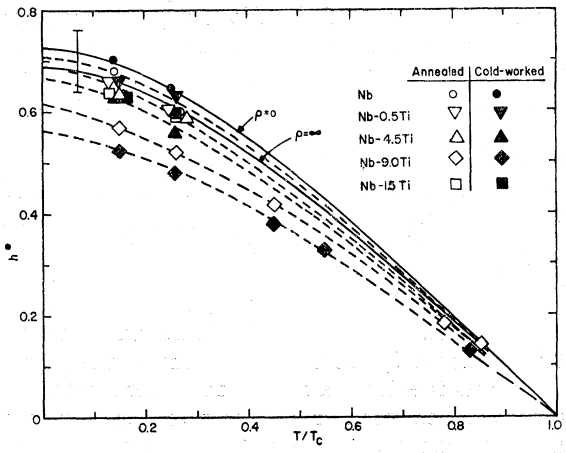

FIG. 11. The upper critical field H_{c2}, normalized to a slope dH_{c2}/dt equal to -1 at $t=1$. The two solid lines are from the work of Helfand and Werthamer for the pure limit and for the dirty limit. Curves for the low titanium alloys have been indicated by the dashed lines where there is sufficient separation to show them. Data are shown for two temperatures. The exact shapes are obtainable from Fig. 3. The error bar is typical and represents mainly the uncertainty in measuring the slope at $t=1$.

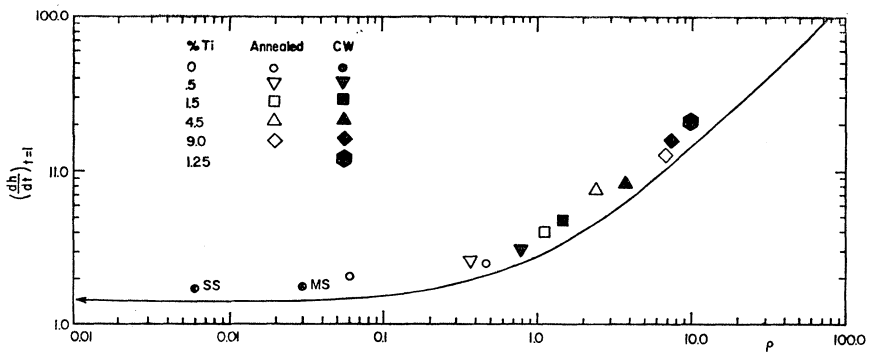

FIG. 12. The normalized slope of the upper critical field at $T_c(dh/dt)_{t=1}$ for all specimens. The points FSS and MS are taken from the work of Finnemore, Stromberg, and Swenson and McConville and Serin, respectively. The solid line gives the theoretical results of Werthamer and Helfand. The labeled points are plotted with ρ calculated from Eq. (7). See text.

$\rho\sim 1$ that was obtained by Eilenberger for the cases with appreciable p-wave scattering is confirmed experimentally is not clear because the experimental uncertainty is too large to permit a definitive conclusion about this very small effect. Near the clean limit our results extrapolate through the data of McConville and Serin and of Finnemore, Stromberg, and Swenson, whose data also appear in Fig. 9.

The values of $\kappa_1(0.1)/\kappa(1)$ for the cold-worked alloys lie higher than the corresponding annealed alloys as can be seen by comparing similarly shaped points in Fig. 9. The data on the worked alloys, of course, appear at larger ρ because their resistivities are increased by working. It is not clear why higher values of $\kappa_1(0.1)/\kappa$ are observed. The elastic strain associated with the high dislocation density produced by cold working is expected to increase H_c slightly, but probably not enough, nor with the right temperature dependence, to account for this effect.[19,20] We have not been able to identify any possible misinterpretation of the highly irreversible data that would give this result as a spurious effect.

Implicit in the theoretical curves plotted in Fig. 9 is the BCS relation for $H_c(t)$. However, our experimental measurements of $H_c(t)$ show that the low-temperature limits $H_c(0)_{\text{meas}}$ are all about 17% higher than the BCS values $H(0)_{\text{BCS}}$ calculated from T_c. (See Table I.) Thus the main effect on the theoretical $\kappa_1(0.10)/\kappa(1)$ of replacing the BCS values of $H_c(t)$ with the measured values can be found by simply dividing the theoretical values in Fig. 9 by the ratio $H_c(0)_{\text{meas}}/H_c(0)_{\text{BCS}}\cong 1.17$. This widens the discrepancy between theory and experiment.

In Fig. 10 the variation of $\kappa_2(0.10)/\kappa(1)$ is shown as a function of ρ, along with Eilenberger's results for this quantity. Qualitative agreement of the shapes of the curves is evident although the experimental values show a much stronger temperature dependence over the whole range of ρ but especially at low temperatures. Again the discrepancy is increased if the BCS values of $H_c(t)$ are replaced by the experimental results.

A normalization of experimental data on $H_{c2}(t)$ that does not explicitly involve $H_c(t)$ can be accomplished by plotting a reduced upper critical field $h^*=H_{c2}(t)/(-dH_{c2}/dt)_{t=1}$ against temperature as advocated by Werthamer and Helfand. In Fig. 11 our data are compared with the calculations of Werthamer and Helfand for $\rho=0$ (clean limit) and $\rho=\infty$ (dirty limit). The dependence of h^* on ρ is weak, and the data agree with theory within experimental error, except for the highest titanium alloy, which should lie lower as observed because of paramagnetic effects.[11]

Since this normalization of the temperature dependence of $H_{c2}(t)$ agrees well with the theoretical calculations while $\kappa_1(t)/\kappa$ and $\kappa_2(t)/\kappa$ do not, attention is focused on the normalization parameter $(dH_{c2}/dt)_{t=1}$. Helfand and Werthamer[10] define a normalized field h such that

$$\left(\frac{dh}{dt}\right)_{t=1}=\frac{0.5807}{\kappa_0 H_c(0)}\left(\frac{dH_{c2}}{dt}\right)_{t=1}$$

$$=\frac{0.5807}{\kappa_0}\frac{T_c}{H_c(0)}\left(\frac{dH_{c2}}{dT}\right)_{t=1}, \qquad (12)$$

where $(dh/dt)_{t=1}$ is given as a function of ρ only. It varies from a limiting value 1.426 in the clean limit to a linear dependence $(dh/dt)_{t=1}=1.216\rho$ in the dirty limit. Using the measured values of $H_c(0)$ and $(dH_{c2}/dt)_{t=1}$, and the calculated values of κ_0 this comparison is made in Fig. 12 as a function of ρ. The general shape of the theoretical curve is in excellent agreement with the data, but precise comparison hinges on the choice of values of ρ. The values of ρ calculated from the residual resistance ρ_n and κ_0 as tabulated in column 6 of Table IV were used in plotting the points in Fig. 12. However, these values are not entirely consistent with the assumptions underlying the calculation of Helfand and Werthamer leading to Eq. (12) since a factor $(S/S_f)^2$ was introduced to make κ_0 consistent with experiment in the clean limit. A good fit using these values of ρ would be obtained by raising the theoretical curve about 25%. Use of values of ρ calculated from Eq. (10) using only measured values of κ, γ, and ρ_n as given in column 9 of Table IV increases the discrepancy near the dirty limit. Use of the values of ρ calculated from experimental values of κ and calculated κ_0 (column 10 of Table IV) improves the agreement in the dirty limit, but the theoretical curve still appears to be

[19] W. W. Webb, Phys. Rev. Letters **11**, 191 (1963).
[20] G. A. Alers and D. L. Waldorf, Phys. Rev. Letters **6**, 677 (1961).

too low. Measured values of $H_c(0)$, and implicitly T_c, have been used in calculating $(dh/dt)_{t=1}$ instead of the prescribed BCS values. Replacement with the BCS values of $H_c(0)$ raises the experimental points about 17% and increases the discrepancy.

DISCUSSION AND CONCLUSION

Our results show that the temperature and mean free path variations of the magnetic properties of type-II superconductors near the upper critical field are qualitatively described by recent calculations in the weak coupling limit based on Gor'kov's generalization of Ginzburg-Landau theory. The quantitative discrepancies in the temperature dependences seem to be inherent in the description of the superconductor near T_c not merely in the theory for lower temperatures.

One of the most obvious features of the data is in the strong temperature dependence of the generalized Ginzburg-Landau parameters, κ_1 and κ_2. In all the alloys investigated, this variation was some 20–50% larger than predicted, in general agreement with the observations of other workers.[6,7,21–32] Hohenberg and Werthamer,[33] considering this discrepancy, have recently suggested that a nonspherical Fermi surface will always lead to a larger value of $H_{c2}(0)$ than spherical Fermi surface in the same system. Although these experiments certainly do not provide adequate confirmation of this suggestion they are consistent with it.

The effect of cold work in enhancing the temperature variation of κ_1 is an interesting complication. The difference can be seen by comparisons in Fig. 6 and Fig. 7, but is even more striking in the dependence on calculated electron mean free path shown in Fig. 9. Of course, it is possible that the resistivity is simply not a good measure of the appropriate average electron mean free path in cold-worked materials. Alternatively, the fact that annealed and cold-worked alloys of the same resistivity differ substantially in their values of $\kappa_1(0.1)/\kappa$ except in the dirty limit suggests that the details of the scattering process are indeed important to the temperature dependence of κ_1 as is illustrated by the Eilenberger calculation of the effects of relatively simple p-wave scattering by impurities.

Although the experimental uncertainties are too large to permit any conclusions regarding the apparent structure in the curves of $\kappa_1(t)$ and $\kappa_2(t)$ there appear to be inflections around $t=0.6$ as can also be seen in the results of McConville and Serin on pure niobium. The calculations of Eilenberger show similar structure.

The normalized values of H_{c2} discussed in Figs. 11 and 12 suggests a route to understanding of the quantitative discrepancies between current theory and experiment. Since the general shape of $H_{c2}(t)$ (see Fig. 11) appears to be adequately accounted for, the main problem seems to be in making the appropriate connection of dH_{c2}/dt at T_c with the impurity parameter ρ in the regime of Ginzburg–Landau theory.

ACKNOWLEDGMENTS

The authors would like to acknowledge useful conversations with Dr. N. R. Werthamer and Dr. Gert Eilenberger, and Professor J. W. Wilkins and Professor N. W. Ashcroft, and would like to thank Professor Clayton Swenson for a copy of his paper on pure niobium prior to publication. We also gratefully acknowledge the financial support of the U. S. Atomic Energy Commission and the use of facilities and services provided by the Advanced Research Projects Agency through the Materials Science Center at Cornell University.

---

[21] T. McConville and B. Serin, Phys. Rev. **140**, A1169 (1965).
[22] L. C. Skinner II, R. M. Rose, and J. Wulff, J. Appl. Phys. **37**, 2491 (1966).
[23] D. K. Finnemore, T. F. Stromberg, and C. A. Swenson, Phys. Rev. **149**, 231 (1966).
[24] E. S. Rosenblum, S. H. Autler, and K. H. Gooen, Rev. Mod. Phys. **36**, 77 (1964).
[25] Ray Radebaugh and P. H. Keesom, Phys. Rev. **149**, 217 (1966).
[26] A. R. Strnad and Y. B. Kim, in *Proceedings of the Symposium on Quantum Fluids, University of Sussex, 1965* (North-Holland Publishing Company, Amsterdam, 1966).
[27] Y. Shapira and L. J. Neuringer, Phys. Rev. **140**, A1638 (1965).
[28] C. K. Jones, J. K. Hulm, and B. S. Chandrasekhar, Rev. Mod. Phys. **36**, 74 (1964).
[29] W. C. H. Joiner and R. D. Blaugher, Rev. Mod. Phys. **36**, 67 (1964).
[30] T. Kinsel, E. A. Lynton, and B. Serin, Rev. Mod. Phys. **36**, 105 (1964).
[31] G. Bon Mardion, B. B. Goodman, and A. Lacaze, J. Phys. Chem. Solids **26**, 1143 (1965).
[32] W. A. Fietz, Rev. Sci. Instr. **36**, 1621 (1965).
[33] P. C. Hohenberg and N. R. Werthamer, Phys. Rev. (to be published).